Supplemental Material: Wide Effective Work-Function Tuning of Al/SiO_2/Si Junction Achieved with Graphene Interlayer at Al/SiO_2 Interface

Wonho Song,[1] Jung-Yong Lee,[2] Junhyung Kim,[1] Jinyoung Park,[1] Jaehyeong Jo,[1] Eunseok Hyun,[1] Jiwan Kim,[1] Daejin Eom,[3] Gahyun Choi,[3,*] and Kibog Park[1,4,†]

[1]Department of Physics, Ulsan National Institute of Science and Technology (UNIST), Ulsan 44919, Republic of Korea
[2]Korea Development Bank, Seoul 07242, Republic of Korea
[3]Korea Research Institute of Standards and Science (KRISS), Daejeon 34113, Republic of Korea
[4]Department of Electrical Engineering, Ulsan National Institute of Science and Technology (UNIST), Ulsan 44919, Republic of Korea

FORMALISM FOR ANALYTICAL ELECTROSTATIC MODELING

The flat-band diagram of metal/oxide/semiconductor (MOS) and metal/graphene/oxide/semiconductor (MGOS) junctions are calculated by solving one-dimensional Poisson equation with the charge distributions shown in Fig. S1(a) and (b). The parameters used in the calculation are defined as follows, Q_m: Metal surface charge density, Q_{ox}: Fixed oxide charge density at the SiO_2/n-Si interface, Q_g: Doping charge density of graphene, Q_i: Dipole charge density formed by interaction between metal and graphene, Q_s: Trap charge density on the graphene-side SiO_2 surface making the graphene layer p-type doped, $t_{ox}(= 30$ nm): Thickness of SiO_2 layer, $d_1(= 3.3$ Å [1]): Gap between metal and graphene, $d_2(= 5$ Å): Gap between graphene and SiO_2, $\phi_m(= 4.08$ eV for Al [2], 5.65 eV for Pt [3]): Metal work-function, $\chi_s(= 4.05$ eV [4]): Electron affinity of Si, $V_n(= (k_BT/q)\ln(N_C/N_D))$: Voltage difference between conduction band minimum and Fermi level of n-Si, V_{FB}: Flat-band voltage, $\phi_g(= 4.50$ eV [5]):

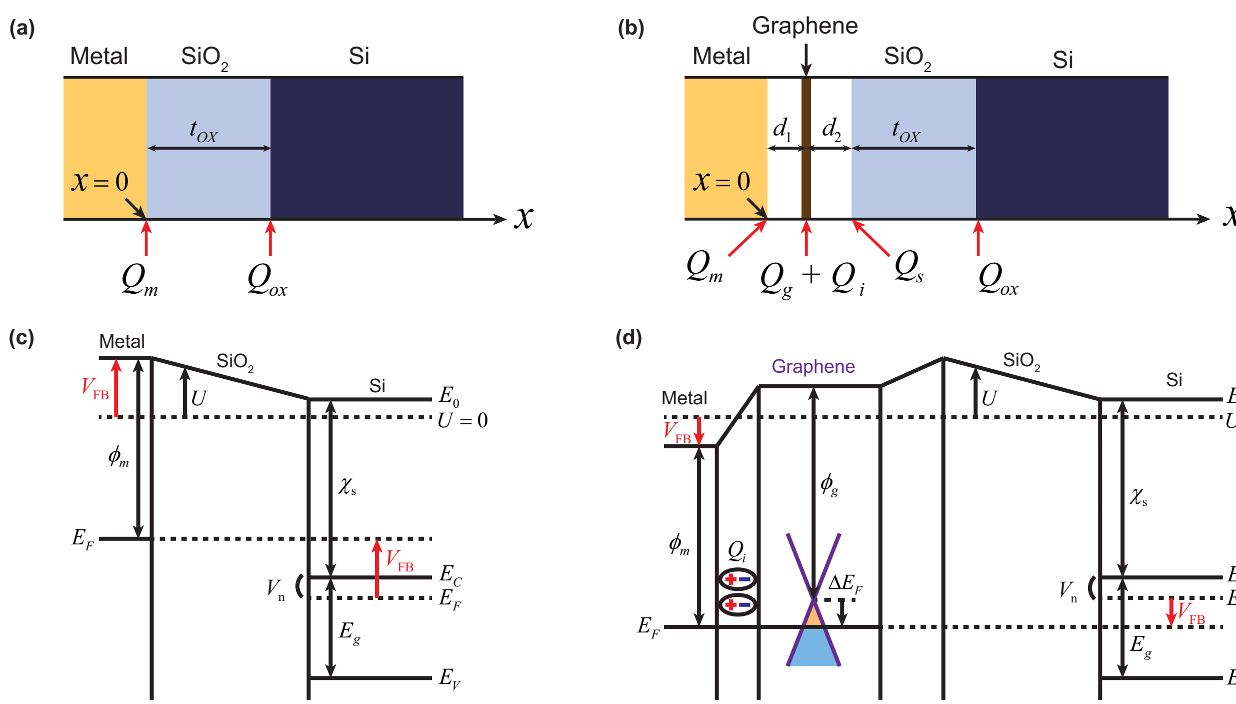

FIG. S1: Spatial charge distributions and flat-band diagrams for metal/SiO_2/n-Si ((a), (c)) and metal/graphene/SiO_2/n-Si ((b), (d)) junctions. The band diagrams were drawn for the case of Al metal electrodes.

Work-function of undoped graphene, ΔE_F: Energy difference between Dirac point and Fermi level of graphene, k_B: Boltzmann constant, $N_C(= 2.82 \times 10^{19}$ cm^{-3} [4]): Conduction band effective density of states, ϵ_0: Vacuum permittivity, $\epsilon_s(= 11.7$ [4]): Dielectric constant of Si, $\epsilon_{ox}(= 3.9$ [6]): Dielectric constant of SiO_2, $N_D(= 3 \times 10^{15}$ cm^{-3}): Donor concentration of n-Si, q: Elementary charge, $\hbar$: Reduced Planck constant, $v_F(= 10^6$ m/s [5]): Fermi velocity of graphene.

All of known constants used in the calculation are obtained from literature [1–6]. At the flat-band voltages, depletion or accumulation charge densities of both MOS and MGOS junctions are zero. Hence, it is reasonable to assume the charge density distributions across junctions as shown in Fig. S1. First, in the MOS junction, the electric field $E(x)$ and potential $U(x)$ can be calculated by using the Gauss' law with the charge distributions shown in Fig. S1(a) as follows.

$$E(x) = \begin{cases} \frac{1}{\epsilon_{ox}\epsilon_0} Q_m & (0 \le x < t_{ox}) \\ 0 & (t_{ox} \le x) \end{cases} \tag{1}$$

$$U(x) = \begin{cases} V_{FB} - \frac{1}{\epsilon_{ox}\epsilon_0} Q_m x & (0 \le x < t_{ox}) \\ V_{FB} - \frac{1}{\epsilon_{ox}\epsilon_0} Q_m t_{ox} & (t_{ox} \le x) \end{cases} \tag{2}$$

Also, the net charge density across the junction should be zero because the electric fields at both ends of junction are zero. That is, $Q_m + Q_{ox} = 0$. By the way, the electrostatic potential change across the junction can be reflected on the potential at $x = t_{ox}$, $U(t_{ox}) = \phi_m - \chi_s - V_n$. By using the potential at $x = t_{ox}$ as the boundary condition of eq. 2, we can obtain the relation between Q_{ox} and V_{FB}.

$$\begin{aligned} \phi_m - \chi_s - V_n &= V_{FB} - \frac{1}{\epsilon_{ox}\epsilon_0} Q_m t_{ox} \\ Q_{ox} &= \frac{\epsilon_{ox}\epsilon_0}{t_{ox}} (\phi_m - \chi_s - V_n - V_{FB}) \end{aligned} \tag{3}$$

Based on the V_{FB} extracted from the C-V curves of MOS junction, the Q_{ox} for the substrate used in this experiment is found to be $9.02 \pm 1.02 \times 10^{-8}$ C/cm^2. Here, it is reasonable to assume that the Q_{ox} obtained for MOS junction is identical to that of MGOS junction because both junctions are fabricated on the same SiO_2/Si substrate and differentiated only by the existence of graphene interlayer. Hence, we used $Q_{ox} = 9.02 \pm 1.02 \times 10^{-8}$ C/cm^2 also to calculate the $E(x)$ and $U(x)$ for MGOS junctions with the charge distributions shown in Fig. S1(b).

$$E(x) = \begin{cases} \frac{1}{\epsilon_0} Q_m & (0 \le x < d_1) \\ \frac{1}{\epsilon_0}(Q_m + Q_g + Q_i) & (d_1 \le x < d_1 + d_2) \\ \frac{1}{\epsilon_{ox}\epsilon_0}(Q_m + Q_g + Q_i + Q_s) & (d_1 + d_2 \le x < d_1 + d_2 + t_{ox}) \\ 0 & (d_1 + d_2 + t_{ox} \le x) \end{cases} \tag{4}$$

$$U(x) = \begin{cases} V_{FB} - \frac{1}{\epsilon_0} Q_m x & (0 \le x < d_1) \\ V_{FB} - \frac{1}{\epsilon_0} Q_m d_1 - \frac{1}{\epsilon_0}(Q_m + Q_g + Q_i)(x - d_1) & (d_1 \le x < d_1 + d_2) \\ V_{FB} - \frac{1}{\epsilon_0} Q_m d_1 - \frac{1}{\epsilon_0}(Q_m + Q_g + Q_i) d_2 \\ \quad - \frac{1}{\epsilon_{ox}\epsilon_0}(Q_m + Q_g + Q_i + Q_s)(x - d_1 - d_2) & (d_1 + d_2 \le x < d_1 + d_2 + t_{ox}) \\ V_{FB} - \frac{1}{\epsilon_0} Q_m d_1 - \frac{1}{\epsilon_0}(Q_m + Q_g + Q_i) d_2 \\ \quad - \frac{1}{\epsilon_{ox}\epsilon_0}(Q_m + Q_g + Q_i + Q_s) t_{ox} & (d_1 + d_2 + t_{ox} \le x) \end{cases} \tag{5}$$

Similarly to MOS junction, the Q_m can be calculated by using the boundary condition $U(d_1+d_2+t_{ox}) = \phi_m - \chi_s - V_n$ which can be conceived in Fig. S1(d) and the charge neutrality condition $Q_m + Q_g + Q_i + Q_s + Q_{ox} = 0$. From eq. 5,

$$\begin{aligned} \phi_m - \chi_s - V_n &= V_{FB} - \frac{1}{\epsilon_0} Q_m d_1 - \frac{1}{\epsilon_0}(Q_m + Q_g + Q_i) d_2 - \frac{1}{\epsilon_{ox}\epsilon_0}(Q_m + Q_g + Q_i + Q_s) t_{ox} \\ &= V_{FB} - \frac{1}{\epsilon_0} Q_m d_1 + \frac{1}{\epsilon_0}(Q_s + Q_{ox}) d_2 + \frac{1}{\epsilon_{ox}\epsilon_0} Q_{ox} t_{ox} \end{aligned}$$

$$Q_m = \frac{\epsilon_0}{d_1}(V_{FB} - \phi_m + \chi_s + V_n) + \frac{d_2}{d_1}(Q_s + Q_{ox}) + \frac{t_{ox}}{d_1 \epsilon_{ox}} Q_{ox} \tag{6}$$

Here the trap charge density on the SiO_2 surface Q_s = -1.12×10^{-6} C/cm^2 is obtained from the transfer curve of a graphene field effect transistor fabricated on highly p-type doped Si substrate with thermally-grown SiO_2 layer. Q_s is considered not to change in the gate voltage range used in our experiments since the trap states are known to be ~1.5 eV below from the Fermi-level of graphene [7]. Since the metals used in our works are known to form weak bonding with graphene enough to preserve the linear dispersion relation of graphene, the doping charge density of graphene Q_g can be expressed as follows [8].

$$Q_g = \frac{q\Delta E_F |\Delta E_F|}{\pi \hbar^2 v_F^2} \tag{7}$$

From the flat-band diagram drawn in the Fig. S1(d), ΔE_F can be expressed as $V_{FB} + \phi_m - \phi_g - U(d_1)$. Hence, Q_g can be obtained from Q_m by using eqs. 5-7. Then, the interaction dipole charge Q_i can finally be determined by using the charge neutrality condition.

$$\begin{aligned} Q_g &= \frac{q(V_{FB} + \phi_m - \phi_g - U(d_1))|V_{FB} + \phi_m - \phi_g - U(d_1)|}{\pi \hbar^2 v_F^2} \\ &= \frac{q\left(\phi_m - \phi_g + \frac{1}{\epsilon_0} Q_m d_1\right)\left|\phi_m - \phi_g + \frac{1}{\epsilon_0} Q_m d_1\right|}{\pi \hbar^2 v_F^2} \end{aligned} \tag{8}$$

$$\begin{aligned} Q_i &= -Q_m - Q_s - Q_{ox} - Q_g \\ &= -Q_s - Q_{ox} - \frac{\epsilon_0}{d_1}(V_{FB} - \phi_m + \chi_s + V_n) - \frac{d_2}{d_1}(Q_s + Q_{ox}) - \frac{t_{ox}}{d_1 \epsilon_{\mathrm{SiO_2}}} Q_{ox} - Q_g \end{aligned} \tag{9}$$

In Table S1, the charge densities and effective work-functions of MOS and MGOS junctions obtained from the experimentally-measured V_{FB}, Q_s and Q_{ox} are listed. The wide tuning of ϕ_M^e of Al/SiO_2/Si junction with the graphene interlayer appears to originate from negative Q_i. The role of Q_i is supported by the decrease of ϕ_M^e for Pt electrode where Q_i turns out to be positive. These results are consistent with the previous works performed on GaAs Schottky junctions [9].

	Al/SiO_2/Si	Al/G/SiO_2/Si	Pt/SiO_2/Si	Pt/G/SiO_2/Si
V_{FB} (V)	-0.98	0.06	0.57	0.37
Q_{ox} (10^{-8} C/cm^2)	9.02±1.02	9.02±1.02	9.02±1.02	9.02±1.02
Q_m (10^{-6} C/cm^2)	-0.09	1.27	-0.09	-2.12
Q_s (10^{-6} C/cm^2)	-	-1.12	-	-1.12
Q_g (10^{-7} C/cm^2)	-	0.37	-	15.44
Q_i (10^{-7} C/cm^2)	-	-2.85	-	15.98
ϕ_m^e (eV)	3.31	4.35	4.85	4.66

TABLE S1: Charge densities and effective work-functions of metal/SiO_2/n-Si and metal/graphene/SiO_2/n-Si junctions.

THE EFFECT OF INTERACTION DIPOLE LAYER

In order to examine the necessity of Q_i for explaining the change of effective work-function, we have tried to produce the experimental outcomes just by using d_2 as a variable with Q_i excluded. As noted previously, the other parameters can be determined from our own experiments or obtained from literature. Hence, if we substitute $Q_g = -Q_m - Q_s - Q_{ox}$

	Al/G/SiO$_2$/Si		Pt/G/SiO$_2$/Si	
d_2 (Å)	3.9	5.7	3.9	5.7
V_{FB} calculated from eq. 11 (eV)	-0.15	0.06	0.37	0.58

TABLE S2: d_2 bearing the measured V_{FB} of metal/graphene/SiO$_2$/n-Si junctions without the Q_i. Red-colored values of V_{FB} are not consistent with the experimental values.

to the Eq. (7), the following quadratic equation for Q_m can be obtained.

$$-Q_m - Q_s - Q_{ox} = \frac{q\left(\phi_m - \phi_g + \frac{1}{\epsilon_0}Q_m d_1\right)\left|\phi_m - \phi_g + \frac{1}{\epsilon_0}Q_m d_1\right|}{\pi\hbar^2 v_F^2} \tag{10}$$

$$\frac{d_1}{\epsilon_0}Q_m^2 + \left[\frac{2d_1}{\epsilon_0}(\phi_m - \phi_g) \pm \frac{\pi\hbar^2 v_F^2}{q}\right]Q_m + (\phi_m - \phi_g)^2 \pm \frac{\pi\hbar^2 v_F^2}{q}(Q_s + Q_{ox}) = 0 \tag{11}$$

Here, $\pm$ sign corresponds to the case of $\Delta E_F \geq 0$ and $\Delta E_F < 0$, respectively. By solving second-order equation for Q_m, four different values of Q_m can be obtained. Among them, we can choose the one that makes the sign of $Q_g(= -Q_m - Q_s - Q_{ox})$ identical to that of ΔE_F. Also, corresponding V_{FB} can be calculated by substituting the Q_m to eq. 6. It is reduced to

$$V_{FB} = \frac{1}{\epsilon_o}Q_m d_1 - \frac{1}{\epsilon_0}(Q_s + Q_{ox})d_2 - \frac{1}{\epsilon_{ox}\epsilon_0}Q_{ox}t_{ox} + \phi_m - \chi_s - V_n \tag{12}$$

As mentioned previously, V_{FB} for Al/graphene/SiO$_2$/Si junction is measured to be 0.06 V and that of Pt/graphene/SiO$_2$/Si junction is measured to be 0.37 V. As noticed in Table S2, d_2 needs to be assumed differently between *with* and *without* graphene interlayer to bear the experimentally-measured V_{FB}. However, it is not reasonable to use different values of d_2 because we used the same graphene transfer method for both junctions. Hence, it seems inevitable to assume the existence of Q_i which is supported by the previous study [9]. In our formalism, from eq. 8, the polarity of Q_i can vary depending on the value of d_2. In fact, our approach is NOT accompanied with any reliable experimental method to specify the value of d_2. This is certainly the limitation of our works. By considering this limitation, we have investigated how the polarity of Q_i is related to Q_s and d_2. In the colored area of Figure S2, Q_i is negative for Al and positive for Pt. Here, the red dashed line indicates the Q_s ($= -1.12 \times 10^{-6}$ C/cm^2) obtained from the transfer curve measured on graphene field effect transistor (GFET). As can be seen in the figure, 5 Å of d_2 used in our electrostatic modeling seems positioned well inside the colored area where Q_i is negative for Al and positive for Pt. These polarities of Q_i are consistent with the previous study for the GaAs Schottky junction with the graphene interlayer [9].

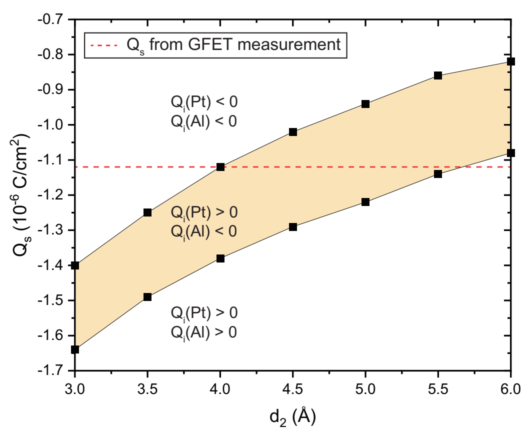

FIG. S2: The range of Q_s which makes the $Q_i < 0$ for Al and $Q_i > 0$ for Pt for the different d_2.

* Electronic address: ghchoi@kriss.re.kr
† Electronic address: kibogpark@unist.ac.kr

[1] P. A., Khomyakov, G. Giovannetti, P. C. Rusu, G. V. Brocks, J. Van den Brink, and P. J. Kelly, Phys. Rev. B **79**, 195425 (2009).
[2] P. A. Tipler and R. A. Llewellyn, *Modern Physics* (W. H. Freeman and Company, New York, 2003), Vol. 5, pp. 130.
[3] H. B. Michaelson, J. Appl. Phys. **48**, 4729 (1977).
[4] B. J. Baliga, *Fundamentals of Power Semiconductor Devices* (Springer, New York, 2010), pp. 24.
[5] Y. J. Yu, Y. Zhao, S. Ryu, L. E. Brus, K. S. Kim, and P. Kim, Nano Lett. **9**, 3430 (2009).
[6] C. M. Tanner, Y. C. Perng, C. Frewin, S. E. Saddow, and J. P. Chang, Appl. Phys. Lett. **91**, 203510 (2007).
[7] H. J. Sung, D. H. Choe, and K. J. Chang, New J. Phys. **16**, 113055 (2014).
[8] A. C. Neto, F. Guinea, N. M. Peres, K. S. Kovoselov, and A. K. Geim, Rev. Mod. Phys. **81**, 109 (2009).
[9] H. H. Yoon, W. Song, S. Jung, J. Kim, K. Mo, G. Choi, H. Y. Jeong, J. H. Lee, and K. Park, ACS Appl. Mater. Interfaces **11**, 47182 (2019).